MANCHESTER 1824
The University of Manchester

The University of Manchester Research

A PXI-based data acquisition system for low-conductivity magnetic induction tomography

Link to publication record in Manchester Research Explorer

Citation for published version (APA):
Mccormick, D., & Armitage, D. (2013). A PXI-based data acquisition system for low-conductivity magnetic induction tomography. In *Proc. 7th World Congress on Industrial Process Tomography* (pp. 228-237). International Society for Industrial Process Tomography.

Published in:
Proc. 7th World Congress on Industrial Process Tomography

Citing this paper
Please note that where the full-text provided on Manchester Research Explorer is the Author Accepted Manuscript or Proof version this may differ from the final Published version. If citing, it is advised that you check and use the publisher's definitive version.

General rights
Copyright and moral rights for the publications made accessible in the Research Explorer are retained by the authors and/or other copyright owners and it is a condition of accessing publications that users recognise and abide by the legal requirements associated with these rights.

Takedown policy
If you believe that this document breaches copyright please refer to the University of Manchester's Takedown Procedures [http://man.ac.uk/04Y6Bo] or contact uml.scholarlycommunications@manchester.ac.uk providing relevant details, so we can investigate your claim.

OPEN ACCESS

Download date:30. Jun. 2022

A PXI-based data acquisition system for low-conductivity magnetic induction tomography

D. McCormick, D.W. Armitage

School of Electrical and Electronic Engineering, University of Manchester, United Kingdom

Abstract

A low-noise, high-stability PXI-based data acquisition system is presented. The system is built using a National Instruments PXI chassis interfacing with a host computer. Data acquisition functionality and system control is implemented using PXI modules programmed using National Instruments LabVIEW software. Data is fetched from a memory buffer on the PXI hardware to the host computer where digital phase sensitive demodulation is used to extract the I- and Q-channels. The system design and integration is discussed to provide a complete description of a generic PXI-based data acquisition system that can be used in low-conductivity magnetic induction tomography applications.

Keywords: data acquisition; low noise; high stability; magnetic induction tomography

1. Introduction

The design of instrumentation for Magnetic Induction Tomography (MIT) requires careful consideration on how to minimise system noise and provide measurement stability. This is particularly important in low-conductivity MIT because the signal of interest is typically several orders of magnitude smaller than the overall signal measured at the detector [1]. At the highest level, the system hardware comprises the coil array, front-end electronics, data acquisition system, and a host computer running control and image reconstruction software [2]. Many low-conductivity MIT systems incorporate bespoke hardware with design objectives focusing on reduction of noise in the signal measurement channels and improving overall monitoring stability of the data acquisition system [3].

This paper details the development of the MITDAQ system, a generic data acquisition architecture built around the PXI (PCI eXtensions for Instrumentation) platform, targeted at low-conductivity MIT applications. A PXI-based data acquisition system interfaces with a host computer via a MXI (Measurement eXtensions for Instrumentation) interface. The MITDAQ system comprises a full signal measurement channel including excitation signal generator and routing, and high-speed multi-channel sampling and digitisation. Acquired data is recorded to a memory buffer on the PXI hardware and is fetched to the host computer where phase sensitive demodulation is used to extract the I- and Q-channels corresponding to the measured electromagnetic properties of the imaged subject. Measurement noise, monitoring stability, and data acquisition throughput is examined to determine the suitability of the system for low-conductivity MIT applications.

2. Magnetic induction tomography

The theory of MIT has been described in the literature [1,4]. The basic arrangement of a single channel measurement for MIT, comprising an excitation coil, a detection coil, and a target dielectric material in the imaging space is illustrated in Fig. 1.

An excitation coil creates a time-varying magnetic field, the excitation field, which permeates into the imaging space. Dielectric materials in the imaging space cause perturbations of the excitation field and eddy currents are induced within the material which creates a second time-varying magnetic field, the induced field. Detection coils situated around the periphery measure the detected field, comprised of both the excitation and induced fields, from which some information about the material can be inferred through signal processing and

image reconstruction. In order to reconstruct images of desired quality, sufficient measurements must be taken through application of differing excitation field patterns.

The case for electromagnetic fields within an inhomogeneous filled imaging space using Maxwell's Equations has been described in [5]. For a constant excitation frequency, the eddy currents induced in the material, which are proportional to the conductivity of the medium, contributes to the imaginary part of the detected field and hence is in quadrature to the excitation field; whereas the displacement current in the material, which is proportional to the permittivity, contributes to the real part of the detected field and hence is in-phase with excitation field. Extraction of both the in-phase and quadrature-phase components of the detected field with respect to the excitation field allows for the independent determination of the permittivity and conductivity of the material.

In low-conductivity MIT the excitation field is significantly larger than the induced field because the induced eddy currents are very small. This presents significant challenges in extracting the induced field from the detected field. Attempts to increase the induced field have focused on increasing the excitation frequencies, typically to frequencies greater than 1MHz, as this improves the signal-to-noise ratio (SNR). The limiting factors in the upper limit of the excitation frequency are the bandwidth of the electronics, considerations of resonances between different coils, and the skin depth of the excitation field in the target material.

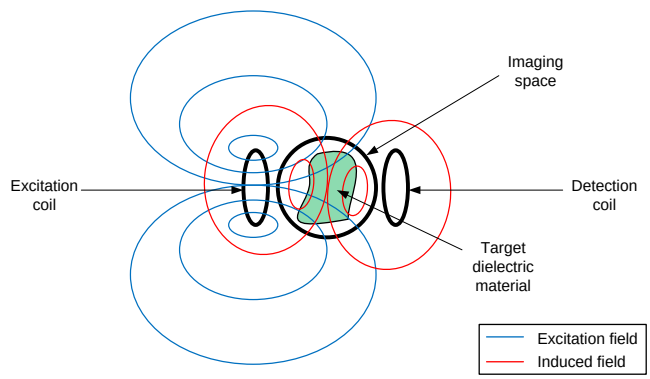

Fig. 1. Basic arrangement of a single channel measurement for MIT.

2.1. Architecture of a MIT system

The general architecture of a MIT system has been outlined in [6]. The design of several low-conductivity MIT systems have been reported in [7-8]. Although there are implementation differences, the general architecture of systems described in the literature is as illustrated in Fig. 2.

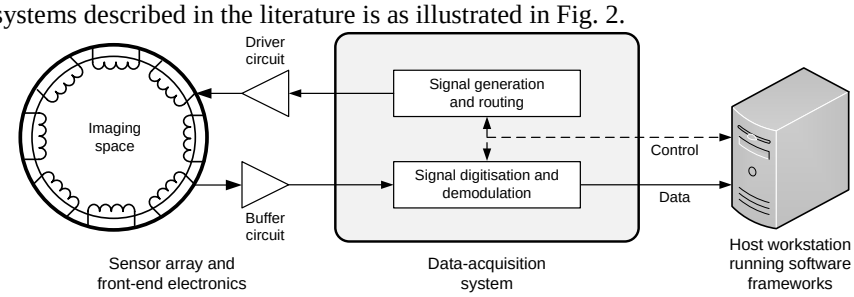

Fig. 2. General architecture of a MIT system illustrating the different sub-systems and interfaces.

A typical MIT system can be considered as a modular design comprised of 3 main sub-systems and interfaces:

- **Sensor array and front-end electronics**; comprising a series of excitation and detector coils situated around the imaging space, electromagnetic screening and shielding, and associated coil driver and buffer circuits.
- **Data acquisition system**; comprising the electronics for generating and routing signals to the sensor array, and for demodulating and digitising detected signals for processing.
- **Host computer**; a generic PC running dedicated software including the data acquisition system control software, and image reconstruction algorithms for processing and generating images.

3. The MITDAQ system

The MITDAQ system is a generic architecture that implements the data acquisition system with control and data interface to the host computer. It is built around the PXI platform, a modular instrumentation platform developed by National Instruments (NI) [9]. PXI instrumentation has been used in several MIT systems [10-12] demonstrating multi-channel systems with low system noise and high long-term stability at operating frequencies in excess of 1MHz. Many of these reported systems have used PXI instrumentation for a subset of the core data acquisition functionality, for example high-speed PXI digitisers for sampling and recording acquired data. Reference [13] demonstrates a complete National Instruments based MIT system built using a FlexRIO FPGA module with transceiver and PXI switching bank to implement the signal generation, routing, and data acquisition functionality.

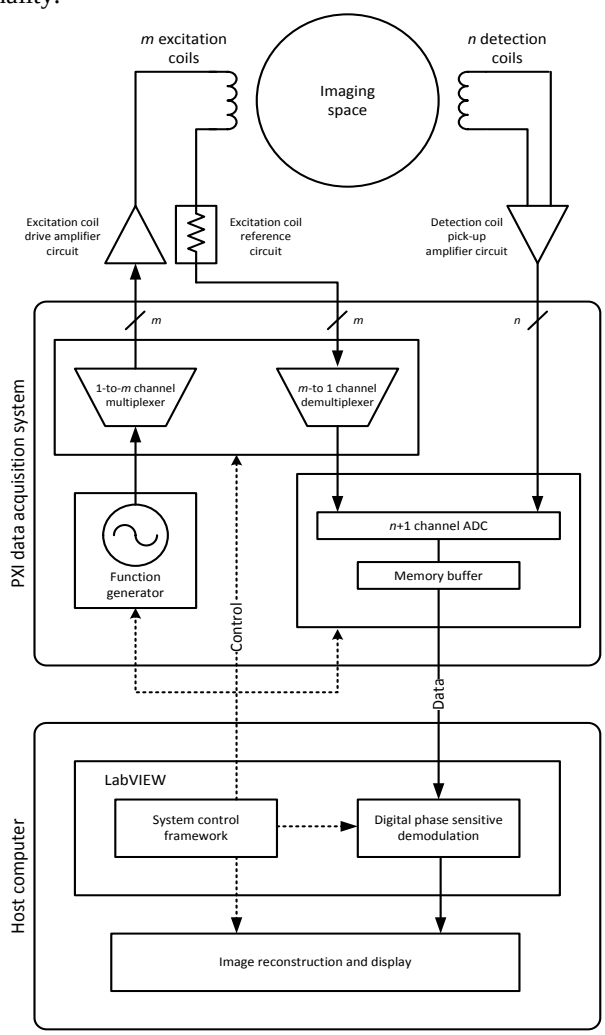

Fig. 3. High-level MITDAQ system architecture.

3.1. System architecture

The high-level MITDAQ system architecture comprising the PXI-based data acquisition system, with *m* excitation channels and *n* detection channels, and a host computer is illustrated in Fig. 3.

3.2. Excitation channel: signal generation and routing

The schematic for the excitation channel signal routing configuration, including the coil drive and reference channels, is shown in Fig. 4.

The data acquisition system is built on a NI PXI-1033 chassis. The chassis comprises the PCI backplane and 3 dedicated PXI modules that implement the core data acquisition functionality:

- NI PXI-5402 function generator
- NI PXI-2593 multiplexer
- NI PXI-5105 multi-channel digitiser

The host computer is a Dell Optiplex 760 with 3GHz Intel Core2Duo processor and 8GB RAM running Windows Vista x64 and LabVIEW 2010 software. The interface between the PXI chassis and host computer is a MXI cable bridging the PCI backplane on the chassis to a micro-PCI card on the PC.

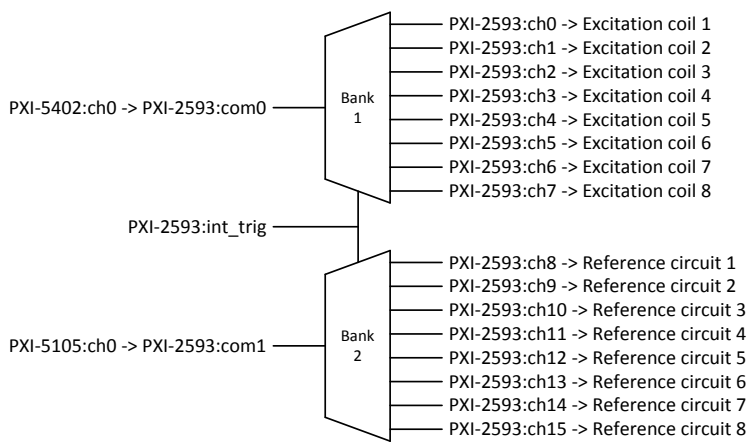

Fig. 4. Signal routing configuration for excitation coil drive and reference channels.

The PXI-5402 operates as a basic enable/disable, single output, sine wave function generator operating up to 20MHz. Signal routing is configured on the PXI-2593 module as a set of back-to-back 8x1 unterminated multiplexer-demultiplexers, implemented as physically-independent, synchronously-switched relay banks. The Bank 1 multiplexer switches the function generator output to up to 8 excitation coils; conversely the Bank 2 demultiplexer switches the corresponding 8 reference channels to a single dedicated master reference channel on the PXI-5105 digitiser. Bank switching is achieved through an internal software trigger on the PXI-2593 module. When switching the switch banks iterate through the predefined scan-list. The trigger initiates the relay switching and monitors the debounced-status of each relay in the banks, typically taking less than 2ms.

3.3. Detection channel: signal digitisation and demodulation

Synchronous multi-channel signal detection and digitisation is implemented on the PXI-5105 module. The digitiser data acquisition cycle performs 3 tasks:

1. **Sample**; where the ADC samples the signals on each channel simultaneously and writes the values to the on-board memory buffer.
2. **Fetch**; involves transferring the sampled data from the on-board memory buffer to the host computer.
3. **Demodulate**; is the extraction of the I- and Q-channels from the acquired data.

A single detection channel, including the pick-up amplifier stage external to the PXI-5105, and the coupling, attenuation and secondary gain circuitry internal to the PXI-5105 module is shown in Fig. 5.

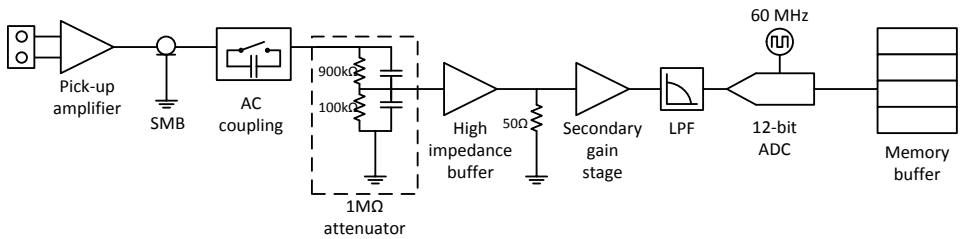

Fig. 5. Schematic of single detection channel.

Each detection channel provides a 1MΩ impedance, AC-coupled, configurable-gain channel designed for general purpose measurements. The secondary gain is controlled by the vertical range of the digitiser channel, which can be extended for larger signals at higher excitation frequencies. With configurable gain of the pick-up amplifiers, variable control of the detection channel gain is possible. Each detection channel measures up to 60MS/s at 14-bit resolution. Digitised data is written to a 128MB memory buffer on the digitiser giving 16MB per channel, which at 2-bytes per sample corresponds to 8,388,608 samples per channel. Data is fetched over the MXI interface to the host computer for off-line signal demodulation. The maximum bandwidth of the MXI interface is 110MB/s limited by the PCI backplane of the PXI-1033 chassis.

Digital Phase Sensitive Demodulation (PSD) is used to extract the in-phase (I) and quadrature-phase (Q) channels from the measured data. For a detected signal $d[n]$, measured with respect to an excitation signal with in-phase component, $i[n]$, and quadrature phase component, $q[n]$, the I- and Q-channels are calculated by Equations (1) and (2) respectively:

$$\mathrm{I} = \sum_{n=0}^{N-1} i[n]d[n] = \sum_{n=0}^{N-1} A_r \sin\left[\frac{2\pi n}{N}\right] A_d \sin\left[\frac{2\pi n}{N} + \phi\right] \tag{1}$$

$$\mathrm{Q} = \sum_{n=0}^{N-1} q[n]d[n] = \sum_{n=0}^{N-1} A_r \cos\left[\frac{2\pi n}{N}\right] A_d \sin\left[\frac{2\pi n}{N} + \phi\right] \tag{2}$$

The digital PSD algorithm is implemented in LabVIEW as a multi-channel VI (Virtual Instrument), which derives the quadrature phase signal from the in-phase signal using a Hilbert Transform, and calls a single channel subVI for each detection channel. The schematic of a single channel digital PSD subVI is shown in Fig. 6.

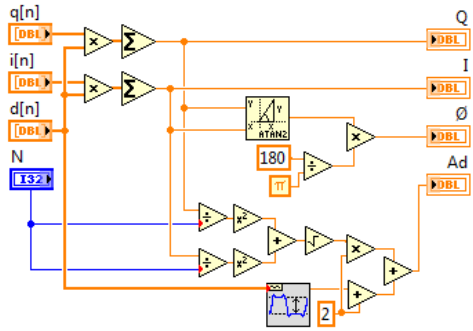

Fig. 6. Schematic of single-channel digital PSD implemented in LabVIEW.

The single channel digital PSD subVI takes quadrature-phase, in-phase, and detected signal, and determines the I-channel, Q-channel, by calculating Equations (1) and (2) directly. From the orthogonally of the I- and Q-channels, the detected signal amplitude, A_d, and phase difference between detected and in-phase reference signal, ϕ, can be calculated. A single pass of the digital PSD subVI constitutes a measurement set for which one I-channel and one Q-channel value for the measured data is calculated.

3.4. System control and integration

The MITDAQ system and control is implemented in LabVIEW on the host computer. The procedure, comprising control of the function generator, multiplexer, and digitiser modules, is illustrated in Fig. 7.

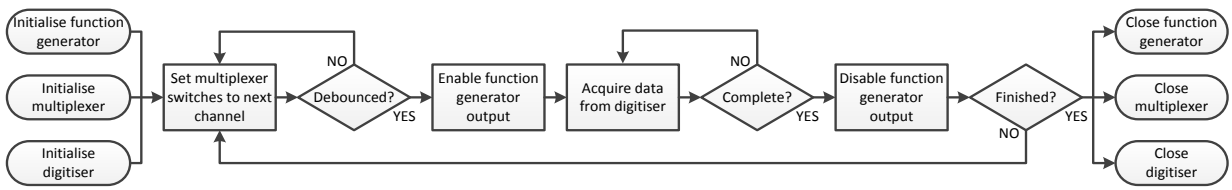

Fig. 7. MITDAQ system integration and control procedure.

Fig. 8 shows the integrated MITDAQ system including PXI hardware, host computer with monitor and peripherals, and coaxial cables routed to the sensor array (not shown).

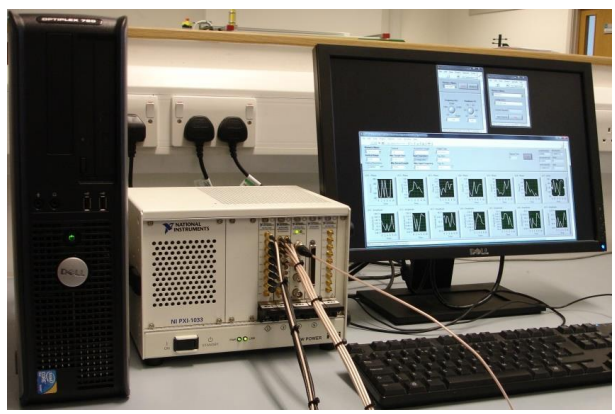

Fig. 8. Integrated MITDAQ system.

4. MITDAQ system testing

Testing the MITDAQ system considers 3 key aspects of the system performance critical for low-conductivity MIT systems: 1) measurement noise, 2) measurement drift and stability, and 3) data acquisition throughput.

4.1. Measurement noise

The digital PSD algorithm was tested in LabVIEW using digitally synthesised signals with added noise. A 17.78mV$_{PK}$ detected signal was demodulated with a 62.5mV$_{PK}$ reference signal at 1MHz sampled at 60MS/s. The calculated RMS phase noise averaged over 100 measurement sets as a function of system SNR and number of measurement samples is shown in Fig. 9 (a) and (b) respectively.

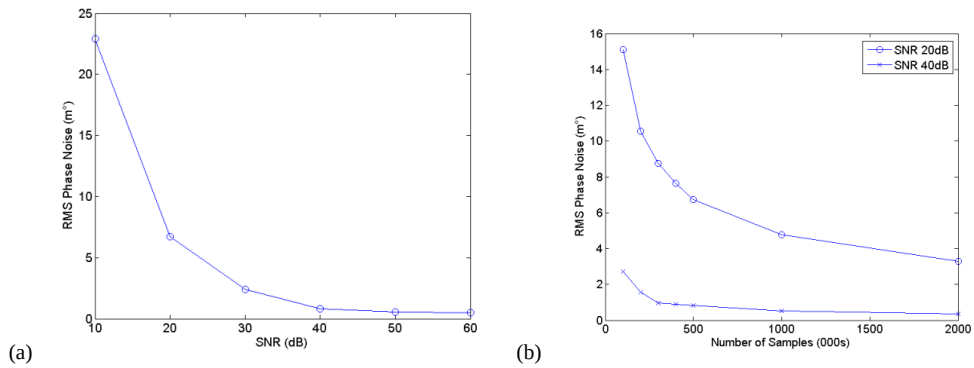

Fig. 9. RMS phase noise as a function of SNR (a), and number of measurement samples for SNR of 20dB and 40dB (b).

Intuitively, the RMS phase noise decreases with increasing system SNR. For 500,000 measurement samples, the RMS phase noise decreases significantly with increasing SNR falling from 22m° at 10dB to 0.8m° at 40dB. Beyond 40dB the RMS phase noise stabilises at less than 0.5m°.

As the number of measurement samples increases the RMS phase noise decreases. This is because the digital PSD is a filter determined by the number of measurement samples for a given sampling rate; i.e. the sampling time. At 60MS/s for a target SNR of 40dB, 100,000 measurement samples, corresponding to a sampling time of 1.67ms, gives a RMS phase noise of around 2.7m°; whereas 500,000 measurement samples, corresponding to a sampling time of 8ms, gives a RMS phase noise of less than 1m°.

To test the measurement noise of the PXI hardware, two measurement channels of the PXI-5105 are driven with synchronous 1MHz 1V$_{PK}$ signals. Measurement sets of 500,000 samples acquired at 60MS/s and 1V$_{PK}$ vertical resolution (full range) are taken each second for 60 seconds after system warm-up. Fig. 10 shows the phase (blue) and amplitude (green) noise normalised to a 90° 1V$_{PK}$ background signal.

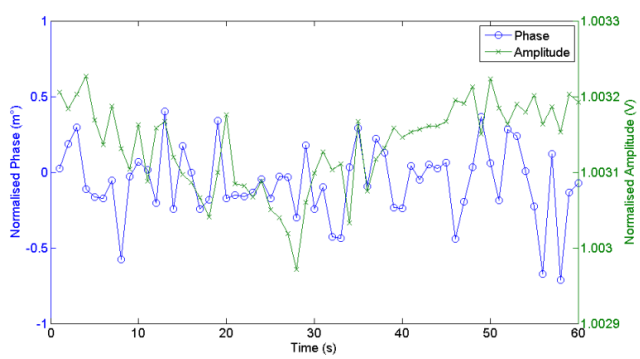

Fig. 10. Measured channel to channel noise.

The measured channel-to-channel RMS phase noise is 0.2m° with peak phase variation of 1.1 m°. The measured channel-to-channel RMS amplitude noise is 57µV giving a SNR of 85dB with peak amplitude variation of 255µV. The results of phase and amplitude noise for the digital PSD algorithm and PXI hardware suggest measurement sets acquired over 8ms at a target system SNR of 40dB would be acceptable for a low-conductivity MIT system requiring high measurement precision.

4.2. Measurement drift and stability

To test the measurement drift and stability of the PXI hardware, two measurement channels of the PXI-5105 are driven with synchronous 1MHz $1V_{PK}$ signals. Measurement sets of 500,000 samples acquired at 60MS/s and $1V_{PK}$ vertical resolution (full range) are taken each second for 2 hours from a cold start. The temperature of the ambient environment is regulated to between 17.5°C and 18.2°C. Fig. 11 shows the phase (blue) and amplitude (green) normalised to the starting phase and amplitude for 2 hours after system power-on.

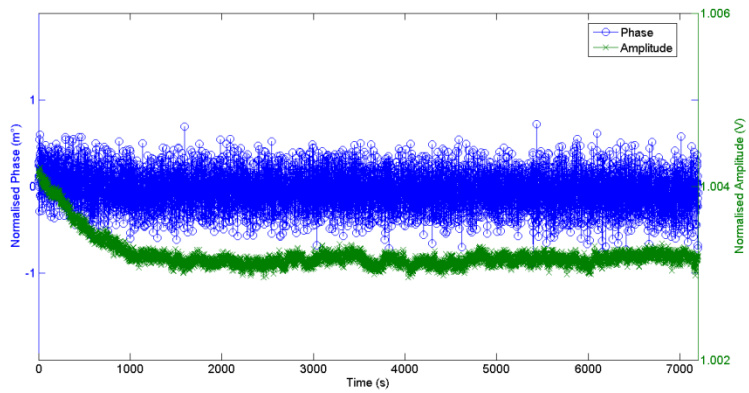

Fig. 11. Normalised phase and amplitude measured over 2 hours from a cold start.

The measured phase does not drift during the 2 hour warm-up. The amplitude drifts by 1.2mV on a $1V_{PK}$ signal, around 0.2%, stabilising after 27 minutes. The observed behavior of the measurement drift is because the PXI-chassis employs active-cooling of the PXI modules which maintains a constant temperature of the internal electronics independent of variations in the external ambient environment, thus limiting thermal drift.

4.3. Data acquisition throughput

The data acquisition throughput describes how long it takes for the MITDAQ system to execute the sample, fetch and demodulate data acquisition cycle. Fig. 12 shows the total data acquisition time for a single measurement set as a function of the number of acquired samples and the proportion of the total acquisition time that is dedicated to the sample, fetch, and demodulate tasks.

The data acquisition time is approximately linear as a function of the number of acquired samples. At larger numbers of samples the demodulation execution time is fractionally non-linear because of the overhead of managing the larger acquired dataset on the host computer.

Within the data acquisition cycle, the most time consuming task is the signal demodulation because it is executed sequentially on each of the 7 detection channels with respect to the reference. Parallelising the demodulation for each channel improves the demodulation execution time by around 26%. The most time consuming element of the demodulation is application of the Hilbert Transform to digitally derive the quadrature-phase signal from the measured in-phase reference signal. In-spite of its lengthy execution time, around 27% of the overall demodulate task time, this is the fastest method for obtaining the quadrature-phase reference signal in LabVIEW. A way to eliminate the need for calculating the Hilbert Transform of the reference signal would be to have a separate circuit which independently derives the quadrature-phase reference signal

from the pre-sampled in-phase reference signal; however this would require a further reference channel on the digitiser module.

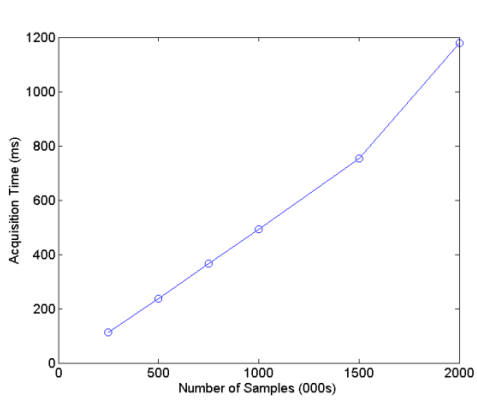

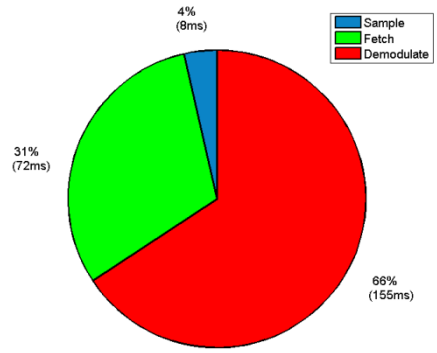

Fig. 12. Data acquisition time as a function of number of samples and the proportion of the total data acquisition time by task.

5. Conclusions

The design and implementation of the MITDAQ system, a generic, low-noise, highly stable PXI-based data acquisition system for low-conductivity MIT has been presented. The system level architecture has been outlined and the design of each PXI module in the system has been described, including the excitation channel signal generation and routing, and the detection channel signal digitisation and demodulation. The overall system control and integration has been discussed.

Testing of the system has considered the measurement noise, the measurement drift and stability, and the data acquisition throughput. The results demonstrate a PXI-based data acquisition system with very low phase and amplitude noise, high measurement stability and low drift over several hours of operation, and measurement sets of 500,000 samples at 60MS/s for a target system SNR of 40dB. The results suggest the MITDAQ system would be suitable for a low-conductivity MIT system requiring a high degree of measurement accuracy and precision.

References

[1] Griffiths, H., 2001. Magnetic induction tomography, Measurement Science & Technology 12, pp. 1126-1131.

[2] Peyton, A.J., Beck, M.S., Borges, A.R., De Oliveira, J.E., Lyon, G.M., Yu, Z.Z, Brown, M.W., Ferrerra, J., 1999. "Development of electromagnetic tomography (EMT) for industrial applications. Part 1: Sensor design and instrumentation," 1st World Congress on Industrial Process Tomography. Buxton, UK, pp. 306-312.

[3] Tapp, H.S., Peyton, A.J., 2003. "A state of the art review of electromagnetic tomography," 3rd World Congress on Industrial Process Tomography. Banff, Canada, p. 340-346.

[4] Korzhenevskii, A.V., Cherepenin, V.A., 1997. Magnetic induction tomography, Journal of Communications Technology and Electronics 42, pp. 506-512.

[5] Korjenevsky, A.V., Cherepenin, V.A., 1999. Progress in realization of magnetic induction tomography, Annals of the New York Academy of Sciences 873, pp. 346-352.

[6] Peyton, A.J., Yu, Z.Z., Lyon, G., Al-Zeibak, S., Ferreira, J., Velez, J., Linhares, F., Borges, A.R., Xiong, H.L., Saunders, N.H., Beck, M.S., 1996. An overview of electromagnetic inductance tomography: description of three different systems, Measurement Science & Technology 7, pp. 261-271.

[7] Rosell-Ferrer, J., Merwa, R., Brunner, P., Scharfetter, H., 2006. A multifrequency magnetic induction tomography system using planar gradiometers: data collection and calibration, Physiological Measurement 27, pp. S271-280.

[8] Vauhkonen, M., Hamsch, M., Igney, C.H., 2008. A measurement system and image reconstruction in magnetic induction tomography, Physiological Measurement 29, pp. S445-S454.

[9] National Instruments, 2013. The PXI Platform, available at: http://www.ni.com/pxi/ (accessed 13th May 2013).

[10] Scharfetter, H., Kostinger, A., Issa, S., 2007. "Spectroscopic 16 channel magnetic induction tomography: The new Graz MIT system," International Conference on Electrical Bioimpedance (ICEBI07), IFMBE Proceedings. Graz, Austria, pp. 452-455.

[11] Wee, H.C., Watson, S., Patz, R., Griffiths, H., Williams, R.J., 2008. "A magnetic induction tomography system with sub-millidegree phase noise and high long-term stability," IFMBE Proceedings of the 4th European Conference of the International Federation for Medical and Biological Engineering. Antwerp, Belgium, pp. 744-747.

[12] Watson, S., Wee, H.C., Patz, R., Williams, R.J., Griffiths, H., 2008. "A method for increasing the phase-measurement stability of Magnetic Induction Tomography systems," IFMBE Proceedings of the 4th European Conference of the International Federation for Medical and Biological Engineering. Antwerp, Belgium, pp. 748-751.

[13] Wei, H.Y., Solemani, M., 2012. Hardware and software design for a National Instrument-based magnetic induction tomography system for prospective biomedical applications, Physiological Measurement 33, pp. 863-879.